



Babol University
Of Medical Sciences

IJMCM, Summer 2025, VOL 14, NO 3

International Journal of Molecular and Cellular Medicine

Journal homepage: www.ijmcm.org



ORIGINAL ARTICLE

Evidence for a TMAO-HULC-miRNA regulatory axis in colorectal cancer cells

Zahra Alighardashi¹ , Mohammad Moradzad² , Sonya Najafpour³ , Zakaria Vahabzadeh^{3,4*}

1. Student Research Committee, Kurdistan University of Medical Sciences, Sanandaj, Iran.

2. Department of Immunology, Faculty of Medicine, Kurdistan University of Medical Sciences, Sanandaj, Iran.

3. Cellular and Molecular Research Center, Research Institute for Health Development, Kurdistan University of Medical Sciences, Sanandaj, Iran.

4. Liver & Digestive Research Center, Research Institute for Health Development, Kurdistan University of Medical Sciences, Sanandaj, Iran.

ARTICLE INFO

Received: 2025/06/1

Revised: 2025/08/2

Accepted: 2025/09/3

*Corresponding:

Zakaria Vahabzadeh

Address:

Kurdistan University of
Medical Sciences,
Faculty of Medicine,
Department of Clinical
Biochemistry

E-mail:

zakariav@gmail.com

ABSTRACT

Colorectal cancer (CRC) is a malignancy with a significant global disease burden. Trimethylamine N-oxide (TMAO), a gut microbiota-derived metabolite, has been implicated in tumorigenesis. The oncogenic long non-coding RNA highly upregulated in liver cancer (HULC) plays a pivotal role in CRC progression. However, the exact molecular mechanism of HULC and its correlation with TMAO in CRC pathogenesis has remained unclear. This study tested whether TMAO regulates HULC and whether HULC mediates changes in selected miRNAs relevant to CRC.

Caco-2 cells were treated with TMAO (300 μ M, 24 h) and HULC expression was quantified by RT-qPCR. HULC was transiently silenced using CRISPR/Cas13 (CasRx) and the expression of candidate downstream miRNAs (miR-21-5p, miR-200a-3p and miR-34a-5p) was measured by stem-loop RT-qPCR. Data are presented as mean \pm SD of at least three independent biological replicates. Group differences were analyzed by ANOVA with appropriate post-hoc testing.

TMAO treatment significantly increased HULC expression in Caco-2 cells. TMAO also elevated miR-21-5p and miR-200a-3p levels; these increases were attenuated when HULC was silenced. miR-34a-5p expression was not significantly affected by TMAO or by HULC knockdown.

This study demonstrates that TMAO upregulates the oncogenic lncRNA HULC, and this upregulation is associated with increases the expression of miR-21-5p and miR-200a-3p. These findings reveal a TMAO-HULC signaling axis that positively influences the levels of oncogenic miRNAs. However, since a single cell line model was used in this study, it needs for further investigation across diverse CRC cell lines to confirm its generalizability.

Keywords: CRISPR/Cas13, CRC, HULC, TMAO, miRNA

Cite this article: Alighardashi Z, et al. Evidence for a TMAO-HULC-miRNA regulatory axis in colorectal cancer cells. International Journal of Molecular and Cellular Medicine. 2025; 14 (3):0 - 0. DOI: 0



© The Author(s).

Publisher: Babol University of Medical Sciences

This work is published as an open access article distributed under the terms of the Creative Commons Attribution 4.0 License (<http://creativecommons.org/licenses/by-nc/4/>). Non-commercial uses of the work are permitted, provided the original work is properly cited.

Introduction

Colorectal cancer (CRC) is one of the most common and aggressive human malignancies worldwide. In addition, it is the third most prevalent cancer in both men and women and the second leading cause of cancer-related death worldwide (1-3). Despite considerable advances in the diagnosis and treatment of CRC, the overall mortality rate of CRC remains high, because the tumor is often well-advanced and rapidly progressed at the time of diagnosis (4). Cell proliferation, apoptosis, differentiation, and metastasis are all involved in the initiation and progression of epithelial cell cancers (5, 6). Therefore, a thorough understanding of CRC pathogenesis at the molecular level will be required to develop better approaches for CRC prevention and early diagnosis.

Trimethylamine N-oxide (TMAO) is a gut microbiota-derived metabolite that is generated from the metabolism of dietary choline, phosphatidylcholine (PC), betaine, and L-carnitine (7). It has been linked to the pathogenesis of inflammation in various diseases such as atherosclerosis, non-alcoholic fatty liver disease, diabetes, obesity, multiple sclerosis, and CRC (8, 9). TMAO is involved in CRC progression, and metastasis through different mechanisms, such as inflammation, DNA damage, and activating cancer-causing signaling pathways (10). TMAO can cause inflammation by activating the p38MAPK pathway, a vital signaling pathway in inflammation, which is activated by different stimuli such as cytokines, growth factors, and stress signals (11).

The human genome contains approximately 2% of protein-coding genes and several non-coding RNAs (ncRNAs) (12). Long non-coding RNAs (lncRNAs) are a class of ncRNAs (>200 nucleotides in length) that are not translated into proteins, but can modulate gene expression through various mechanisms at both transcriptional and post-transcriptional levels. They have been reported to play key roles in various cellular processes, including proliferation, differentiation, migration, apoptosis, and invasion (13-15). Additionally, the dysregulation of various lncRNAs has been observed in the tumorigenesis of several human malignancies, including CRC, and they have been shown to have either oncogenic or tumor-suppressive functions (16, 17). Highly up-regulated in liver cancer (HULC) is a lncRNA that is up-regulated in CRC, pancreatic cancer, hepatocellular carcinoma,

and osteosarcoma, which may function as an oncogene by targeting different miRNAs (18-20). However, the biological roles and underlying molecular mechanisms of HULC in CRC tumorigenesis remain unclear. HULC might increase to published evidence, HULC tightly regulates P38MAPK pathway both at mRNA and protein level (21).

MicroRNAs (miRNAs) have been recognized as important regulators of mRNA processing. However, their involvement in disease processes has only recently been extensively studied, with a growing body of research highlighting their roles in carcinogenesis, chemoresistance, metastasis, and epithelial-to-mesenchymal transition (EMT) regulation, and with Colorectal Cancer: Risk Factors, Novel Approaches in Molecular Screening and Treatment (22-24). The overexpression of miR-21-5p has been observed in both tumor tissues and cell lines of CRC patients (25).

It plays a crucial role in regulating tight junction (TJ) proteins like occludin and ZO-1 which maintain the integrity of the intestinal epithelial barrier, thereby influencing its permeability and function (26). It has been shown that miR-21 regulates the p38 MAPK pathway during inflammatory responses following myocardial infarction and viral infections (27, 28). MiR-200a-3p is markedly elevated in CRC, acting as an oncogene by direct inhibition of PTEN, a crucial regulator of the p38 MAPK signaling pathway, to enhance cell proliferation, migration, and invasion, underscoring its pivotal involvement in CRC tumorigenesis (29). miR-34a-5p, a tumor suppressor, is downregulated in CRC, influencing p38 activity and downstream processes such as EMT, apoptosis, and senescence via both p53-dependent and independent mechanism (30, 31).

We hypothesized that TMAO may induce HULC expression, which in turn could influence expression of miR-21-5p and miR-200a-3p. To test this, we examined the effects of TMAO on HULC and these miRNAs in Caco-2 cells and assessed the impact of HULC knockdown on TMAO-mediated miRNA regulation

Methods

Cell culture and treatments

Caco-2 cells were obtained from the Pasteur Institute (Iran) and cultured in high-glucose Dulbecco's Modified Eagle Medium (DMEM)

supplemented with 10% fetal bovine serum (FBS; Gibco), 2 mM L-Glutamine, 100 U/mL penicillin (Gibco), and 100 U/mL streptomycin (Gibco). Cells were maintained in a humidified incubator at 37 °C with 5% CO₂. For all experiments, cells between passage 4 and 15 were used. Cells were grown to 70-90% confluency, harvested, and seeded at a density of 1.0×10^5 cells/well in a 24-well plate for 24 hours. Trimethylamine N-oxide (TMAO) [Sigma Aldrich, CAS Number 1184-78-7] stock was prepared in sterile water and diluted in culture medium to a final concentration of 300 µM. Vehicle controls received an equivalent volume of sterile water added to fresh medium.

The culture media was then removed and replaced with media containing 300 µM TMAO for 24 hours. This concentration was selected based on our previous published research, where we demonstrated that TMAO exerts significant biological effects in various cancer cell lines within this dose range(32, 33). Using a concentration with a proven record of inducing a molecular response allowed us to reliably investigate the novel downstream cascade involving HULC and its miRNA targets in the Caco-2 model. Then the RNA was extracted from the cells and stored at -70°C until PCR analysis.

Measurement of cell viability

MTT assay was used to measure the viability of TMAO treated cells. Briefly, cells were seeded in a 96-well plate at a density of 5×10^3 cells per well in 100 µL of DMEM and incubated at 37°C for 24 hours. The cells were then treated with TMAO for 24 hours. After treatment, 100 µL of 3-(4,5-dimethylthiazol-2-yl)-2,5-diphenyltetrazolium bromide (MTT) solution (Sigma-Aldrich) at a final concentration of (0.5 mg/mL) was added to each well and incubated for an additional 4 hours. The culture medium was then removed, and the insoluble formazan crystals were dissolved by adding 100 µL of DMSO to each well. Finally, the absorbance was measured at 570 nm using a Synergy HT microplate reader (BioTek, Winooski, VT, USA) to determine cell viability. Experiments for cell viability were conducted using at least three independent biological replicates.

HULC-/- knockdown using CRISPR/Cas13 system:

The CRISPR/Cas13 system was designed to specifically target HULC mRNA for degradation. To

validate the technical efficacy of this system, we included two critical controls: a non-targeting gRNA to assess non-specific effects, and a gRNA targeting Annexin A4 (ANXA4) as a technical positive control.

ANXA4 was specifically chosen for this purpose for two key reasons. First, ANXA4 is a gene that is robustly and constitutively expressed in Caco-2 cells, providing a high baseline transcript level that allows for the reliable and easily quantifiable measurement of knockdown efficiency via RT-qPCR. Second, this specific gRNA targeting ANXA4 was validated in our laboratory to consistently yield efficient knockdown, thereby confirming that our entire experimental pipeline—from plasmid transfection to CasRx-mediated mRNA cleavage—was functioning as expected.(34, 35). The guide RNAs (gRNAs) were designed using the sgRNA design tool available at <https://crispr.mit.edu/> and were synthesized by Pishgam company (Tehran, Iran).

The sgRNA was cloned CasRX pre-gRNA cloning backbone (Addgene 109054) that was linearized with BbsI restriction enzyme(36). Moreover, a green fluorescent protein (GFP) reporter was co-expressed from the CasRx plasmid (pcDNA3-EF1a-CasRx-2A-EGFP; Addgene 109049). The efficiency of plasmid delivery was qualitatively validated prior to downstream experiments by confirming widespread GFP expression throughout the cell culture via fluorescence microscopy. The gRNA sequences used in constructing vectors were illustrated in Table1. Plasmids containing sgRNA were transfected into Caco-2 cells with lipofectamine 3000 (Invitrogen, USA) according to the manufacturer's instructions. After transfection, the transfected cells were treated with TMAO (300µM), for 24 hours in different groups.

RNA Extraction and cDNA Synthesis:

The Total RNA Extraction Kit (Cat. No.: A101231, Parstous; Iran) was used to extract RNA from the cells. Briefly, the cells were transferred to a microcentrifuge tube and 750 µL of RL solution was added and mixed well by pipetting. After incubating for 3 minutes at 37°C, 200 µL of chloroform was added. Following centrifugation, the supernatant was transferred to a new microcentrifuge tube and 400 µL of 70% ethanol was added and mixed well by vortexing. The mixture was then placed in a spin column and washed twice. Finally, 50 µL of DEPC-treated water was added to the membrane center of the

spin column, and the column was centrifuged at high speed to elute the RNA. The purified RNA was stored at -70°C for further processing. The cDNA for HULC expression analysis was synthesized using a cDNA Synthesis Kit (Cat No: YT4500). In summary, 500 ng isolated RNA and 1 µL random hexamer were mixed in 13.5 µL DEPC-treated water and incubated for 5 minutes at 70°C. Subsequently, a mixture containing 5x first-strand buffer (4 µL), dNTPs (10 mM; 1 µL), RNasin (40 U/µL; 0.5 µL), and M-MLV (1 µL) was added and incubated at 37°C for 60 minutes. Ultimately, synthesized cDNA was stored at -20°C. To synthesize cDNA for miRNA expression analysis, the BON Stem High Sensitivity MicroRNA 1st Strand cDNA Synthesis kit (Cat. BON001027SL) was utilized, which employs a poly(A) tailing and universal adaptor ligation method. In brief, 500 ng of total RNA and 1 µL of BON-RT adaptor (1 µM) were combined, and RNase-free water was added to a final volume of 13.5 µL. This mixture was incubated at 75°C for 5 minutes, then immediately placed on ice. Subsequently, 1 µL of RT enzyme (1000 U), 2 µL of dNTP (10 mM), and 4 µL of RT buffer were added. The thermal cycling conditions specified in the manufacturer's protocol were then followed.

RT-qPCR

For the RT-qPCR assay, primers were designed by Gene Runner software (Table 2). Gene expression analysis was performed on cDNA synthesized from RNA isolated from each independent biological replicate. For each biological replicate, RT-qPCR was run in technical triplicates. Master Mix 2X HRM (Lot No:148022362) was used in RT-qPCR. A total 20 µL volume of the final reaction was comprised of 2×qPCR

Mastermix (10 µL), 1 µL of forward and reverse primer (10 µM), 2 µL cDNA (10 or 50 ng) and 6 µL ddH₂O. The reactions were run on a Corbett RG-6000 machine (Australia) Real-Time PCR System. The thermal cycling protocol was as follows: an initial enzyme activation at 95 °C for 10 minutes; followed by 40 cycles of denaturation at 95 °C for 15 seconds and a combined annealing and extension step at 60 °C for 60 seconds. Following amplification, a melt curve analysis was performed. The reverse primer was a universal reverse primer provided with the BON Stem kit, which is specific to the universal adaptor sequence added during cDNA synthesis. To normalize the expression levels of HULC and miRNAs, the expression of β-actin and SNORD were respectively, assessed in parallel with the genes of interest. SNORD44 was chosen as the endogenous control for miRNA normalization due to its established stability in Caco-2 cells and its consistent C_q values across all our treatment groups.

Statistical analysis

Gene expression analysis was calculated using the $2^{-\Delta\Delta C_q}$ method (from the mean of technical replicates for each independent biological replicate). Cell viability data from the MTT assay were also analyzed statistically. To compare mean values across the multiple treatment groups a One-Way ANOVA test was used. Following a significant ANOVA result ($P < 0.05$), post-hoc tests (Tukey's Multiple) were conducted to identify specific group differences. R version 4.3.0 was used for statistical analysis and graphs were drawn using Prism (Version 7.0.0). Significance levels were set at $P < 0.05$, denoted as *, with non-significant differences denoted as ns.

Table 1. The gRNAs used in this study

Target Gene	gRNA Sequence (5'-3')	Target Transcript ID	Target Coordinates	Strand	Off-Target Summary (≤ 2 mismatches)
HULC	AAACAAAGAATATTCCGGCCT TTACTTCAGAGTT	NR_004855.3	266-299	+	0 sites
ANXA4	AACAATTAGGCAGCCCTCATC AGTGCCGGCTCC	NM_001153.5	395-425	+	0 sites
Non-targeting	AAACTCACCAGAAGCGTACCA TACTCACGAACAG	N/A	N/A	N/A	N/A

Target coordinates are relative to the specified NCBI RefSeq transcript ID. Off-target analysis was performed using NCBI BLASTn against the human RefSeq RNA database (refseq_rna), summarizing hits to non-target genes with two or fewer mismatches.

Table 2. Primer sequences for RT-qPCR

Target Name	RefSeq Accession ID	Forward Primer (5'→3')	Reverse Primer (5'→3')	Amplicon Size (bp)	Primer T _m (°C)	PCR Efficiency (%)
β-Actin	NM_001101	AGATCATTGCTC CTCCTGAG	CTAAGTCATAGTC CGCCTAG	161	56°C	1.843
HULC	NR_004855.3	ATCTGCAAGCC AGGAAGAGTC	CTTGCTTGATGCT TTGGTCTGT	184	58°C	1.704
SNORD44	NR_002750.2	ATCACTGTAAA ACCGTTCCA	CCAGTCTCAGGGT CCGAGGTATTC	44	58°C	1.802
miR-21-5p	MIMAT0000076	CGCCGTAGCTTA TCAG	CCAGTCTCAGGGT CCGAGGTATTC*	40	60°C	1.763
miR-34a-5p	MIMAT0000255	AGGGTGGCAGT GTCTTA	CCAGTCTCAGGGT CCGAGGTATTC*	39	60°C	1.763
miR-200a-3p	MIMAT0000519	AACGCTAACAC TGTCTGGT	CCAGTCTCAGGGT CCGAGGTATTC*	41	60°C	1.797

Results

Effect of treatments on cell viability

We assessed cytotoxicity by MTT assay after 24 h exposure to TMAO (75 and 300 μM). As shown in Figure 1, both concentrations caused only minor reductions in cell viability relative to untreated controls. The mean cell viability was reduced by 3.21 % at 75 μM TMAO and by 0.19 % at 300 μM TMAO relative to the control. However, this reduction in cell viability did not reach statistical significance (P > 0.05), indicating that TMAO, at these concentrations, does not exert a significant cytotoxic effect on Caco-2

cells within the 24-hour timeframe. Moreover, microscopic examination of the cells revealed no evidence of cell death or morphological changes associated with cytotoxicity following TMAO treatment.

Our initial cell viability experiments tested TMAO at 75 μM and 300 μM over 24 hours, finding no significant cytotoxicity at either concentration. Based on these preliminary data, the 300 μM concentration was selected for the subsequent gene expression studies of HULC and its downstream targets to investigate effects independent of significant cell death or widespread toxicity.

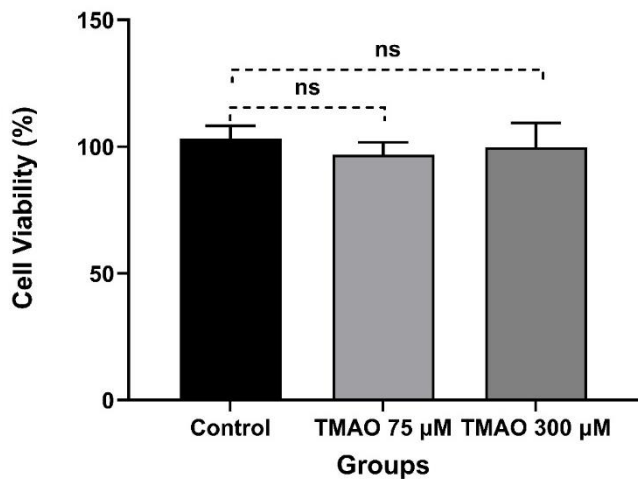


Figure 1. TMAO does not affect the viability of Caco-2 cells. Cell viability was assessed via MTT assay after 24 hours of treatment with 75 μM or 300 μM TMAO. Bars represent the mean ± SD of three independent biological replicates (n=3), with the individual data points for each replicate overlaid on the graph. Statistical analysis was performed using a one-way ANOVA. (ns = not significant, p > 0.05). Absorbance was measured using a Synergy HT microplate reader (BioTek). Raw data are available in Supplementary Table S1.

HULC was successfully knocked down

We confirmed successful HULC knockdown at the gene expression level using RT-qPCR. First, successful transfection of desired plasmid was controlled by visualizing GFP spot (Figure 2). Next, HULC expression was assessed using RT-qPCR. Our results demonstrated that HULC expression was significantly downregulated (P value <0.05), with a calculated mean knockdown efficiency of approximately 56% compared to the control group, indicating it was successfully knocked down. TMAO increased HULC expression in control cells ($p < 0.05$), but this induction was not observed in HULC-silenced cells, consistent with effective knockdown under TMAO exposure (Figure 3).

In contrast, the ANXA4 group and non-targeting control group exhibited no significant changes in HULC expression, confirming the specificity of the knockdown effect. Furthermore, to ensure the selectivity of the knockdown system, the expression of ANXA4 was evaluated across all experimental groups.

Furthermore, to ensure the selectivity of the knockdown system, the expression of ANXA4 was evaluated across all experimental groups. Consistent

with expectations, a significant downregulation of ANXA4 expression was observed exclusively in the group transfected with gRNA targeting ANXA4. The groups with gRNA for HULC and the non-targeting control demonstrated no significant alterations in ANXA4 expression compared to the control group (Figure 4).

These results collectively validate the specificity and efficacy of the HULC knockdown model in Caco-2 cells.

HULC Expression Levels Correlate with miR-21-5p and miR-200a-3p

In comparison with the control group, both miR-21-5p and miR-200a-3p exhibited elevated expression levels when cells were treated with TMAO. However, in the HULC knockdown (KD) group, HULC downregulation led to decreased expression of these miRNAs. Additionally, TMAO could not change miR-21-5p and miR-200a-3p expression in HULC(KD) group. On the other hand, no marked changes were found in miR-34a-5p expression among study groups (Figure 5).

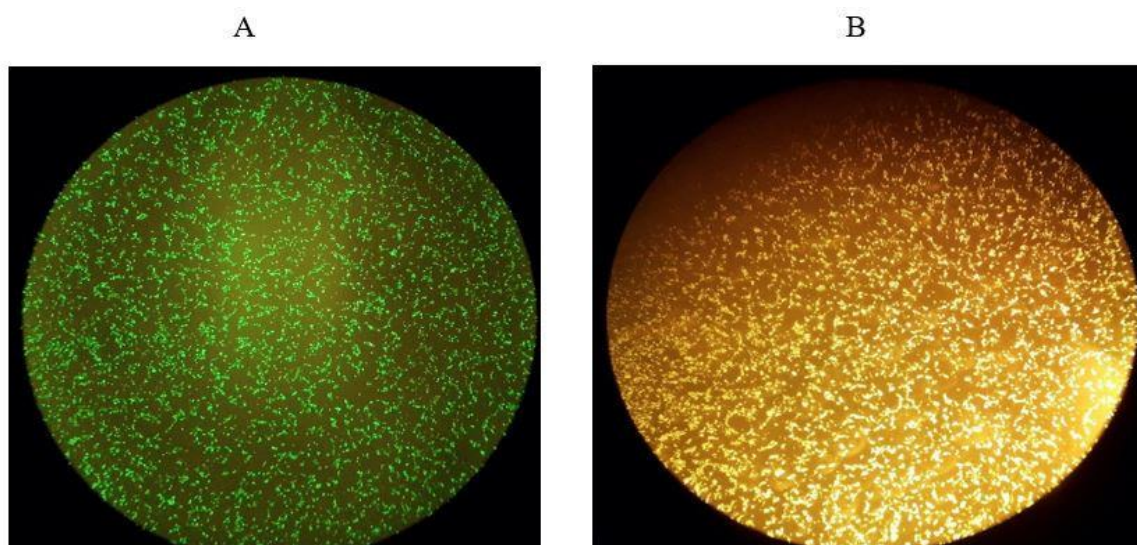


Figure 2. Qualitative validation of transfection efficiency by GFP visualization. Transfection efficiency and GFP expression in Caco-2 cells inspected by inverted fluorescence microscope at 10x objective magnification at 48 hours post-transfection. (A): GFP was observed in cells cultured in the plates that were transfected with CasRX pregRNA expression vector and pcDNA3_EF1a-CasRx-2A-EGFP vector, and (B): shows the same cells with normal visible light.

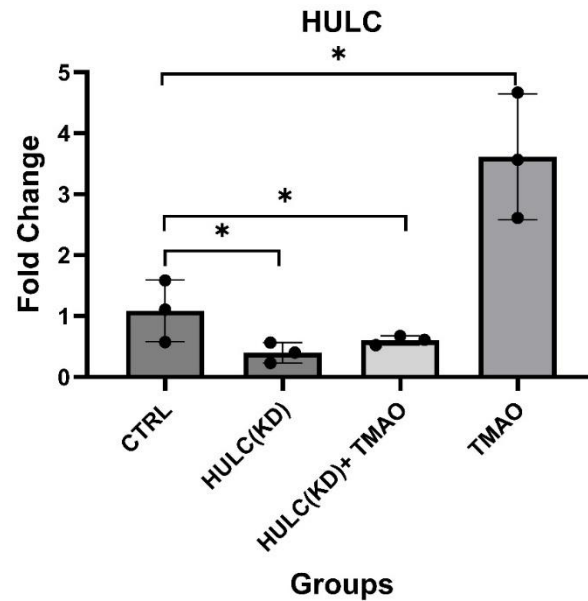


Figure 3. HULC Gene expression across groups. TMAO upregulates HULC expression in Caco-2 cells, an effect that is reversed by HULC knockdown. Data are presented as linear fold change relative to the control group. Bars represent the mean, and error bars represent the standard deviation (SD) of three independent biological replicates (n=3). The individual data points for each replicate are overlaid on the graph. The mean \pm SD fold changes were: CTRL (1.09 ± 0.51), TMAO (3.61 ± 1.03), HULC(KD) (0.40 ± 0.17), and HULC(KD)+TMAO (0.60 ± 0.07). Statistical significance was determined by a one-way ANOVA followed by post-hoc tests. (* $P < 0.05$). The raw data used to generate this figure are available in Supplementary file, raw data for Figure 3.

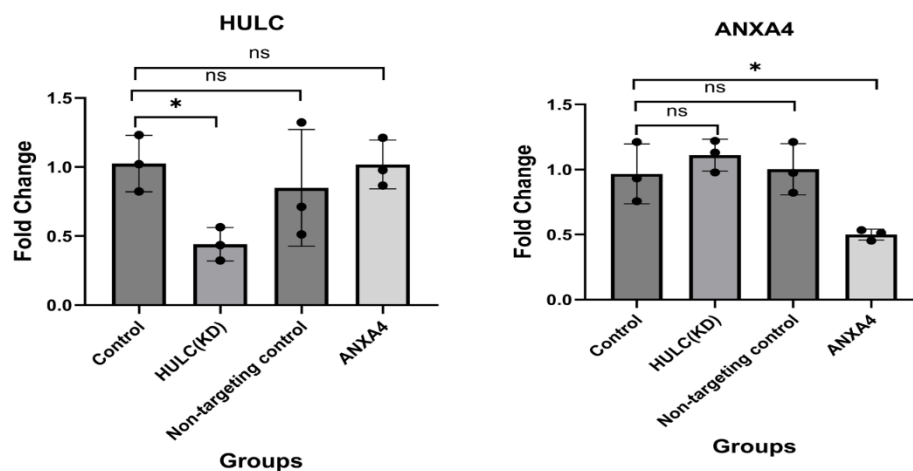


Figure 4. Validation of knockdown specificity for HULC and ANXA4. The figure displays the relative expression of HULC and ANXA4 in response to targeted knockdown of either gene. Data are presented as linear fold change relative to the control group. Bars represent the mean, and error bars represent the standard deviation (SD) of three independent biological replicates (n=3). The individual data points for each replicate are overlaid on the graphs. The mean \pm SD fold changes were as follows: For HULC expression: Control (1.03 ± 0.20), HULC(KD) (0.44 ± 0.12), non-targeting control (0.85 ± 0.42), and ANXA4(KD) (0.18 ± 1.02). For ANXA4 expression: Control (0.97 ± 0.23), HULC(KD) (1.11 ± 0.12), non-targeting control (1.00 ± 0.20), and ANXA4(KD) (0.04 ± 0.5). These results confirm that the knockdown of HULC is specific and does not affect ANXA4 expression, and vice-versa. Abbreviations: HULC(KD), HULC knockdown; ANXA4(KD), ANXA4 knockdown. Statistical significance was determined by a one-way ANOVA followed by post-hoc tests. (* $P < 0.05$). The raw data used to generate this figure are available in Supplementary file, raw data for figure 4.

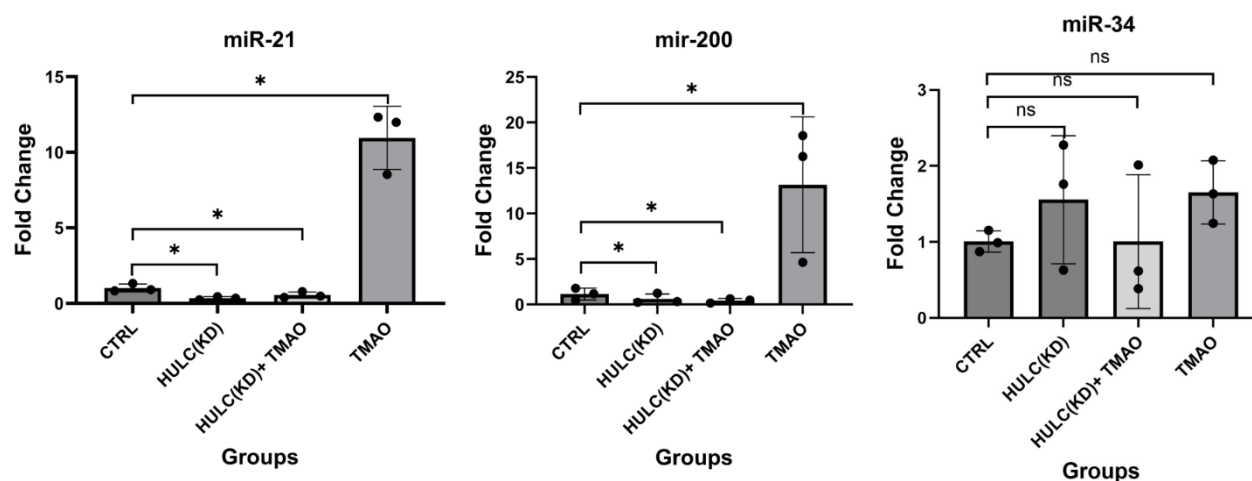


Figure 5. TMAO-induced expression of miR-21-5p and miR-200a-3p is dependent on HULC. The figure displays the relative expression of miR-21-5p, miR-200a-3p, and miR-34a-5p in response to TMAO and/or HULC knockdown. Data are presented as linear fold change relative to the control group. Bars represent the mean, and error bars represent the standard deviation (SD) of three independent biological replicates (n=3). The individual data points for each replicate are overlaid on the graphs. The mean \pm SD fold changes were as follows: For miR-21-5p: CTRL (1.02 ± 0.26), TMAO (10.95 ± 2.09), HULC(KD) (0.34 ± 0.10), and HULC(KD)+TMAO (0.21 ± 0.55). For miR-200a-3p: CTRL (1.15 ± 0.66), TMAO (13.15 ± 7.50), HULC(KD) (0.61 ± 0.55), and HULC(KD)+TMAO (0.25 ± 0.42). For miR-34a-5p: CTRL (1.01 ± 0.14), TMAO (1.65 ± 0.42), HULC(KD) (1.56 ± 0.84), and HULC(KD)+TMAO (0.89 ± 1.01). Abbreviations: CTRL, control; HULC(KD), HULC knockdown; TMAO, Trimethylamine N-oxide. Statistical significance was determined by a one-way ANOVA followed by post-hoc tests. (* $P < 0.05$). The raw data used to generate this figure are available in Supplementary file, raw data for Figure 5.

Discussion

The principal finding of this study is the identification of a novel molecular axis in colorectal cancer cells, whereby the gut microbial metabolite TMAO upregulates the long non-coding RNA HULC. Crucially, these molecular changes occurred in the absence of any significant cytotoxicity, as confirmed by MTT assay, which suggests they arise from specific signaling events rather than a general cellular stress response.

Our data further demonstrate that this increase in HULC is strongly associated with the elevated expression of the oncogenic microRNAs, miR-21-5p and miR-200a-3p, an effect that is reversed upon HULC knockdown. However, it is critical to interpret these findings within the context of the study specific limitations. First, the relationships identified are correlational, as the direct causal mechanisms linking HULC to miRNA expression were not investigated. Second, these observations were made exclusively in the Caco-2 cell line, and the generalizability of this axis to the heterogeneous landscape of CRC requires further

validation. Finally, this work was focused on molecular changes and did not include functional assays or in vivo data to link this signaling axis to phenotypic cancer progression. Therefore, this study serves as a foundational, hypothesis-generating work that uncovers a potential pathway for future mechanistic and functional investigation. In recent years, gut microbiota and its metabolites have captured scholars' attention. TMAO is a gut-liver metabolite that is linked to CRC development. Yang et al. indicated that TMAO causes CRC progression through increasing cell proliferation and angiogenesis(37).

Moreover, Wu et al. demonstrated that TMAO potentially increases cell proliferation and metastasis in hepatocellular carcinoma(38). These findings highlight the role of TMAO in regulatory network associated with cancer. However, there is still little evidence to elucidate molecular mechanisms associated with the tumor activity of TMAO. In the current study, we hypothesized that HULC is a key molecular component of the cellular response to TMAO. Interestingly, our results supported this theory, showing that TMAO significantly elevated HULC expression. This is highly

important because there is a body of evidence to substantiate the oncogenic role of HULC in different cancer types. HULC overexpression contributes to increased cell proliferation and metastatic behavior (EMT elevation), and inhibition of apoptosis in gastric cancer (GC) (39). This is supported by another study that HULC is correlated to GC progression via miR-9-5p (40). Moreover, the upregulation of HULC is related to inhibiting apoptosis in lung cancer through sphingosine kinase 1 (SPHK1) and its downstream PI3K/Akt pathway (41).

Taken together, previous studies did not show a root cause of HULC overexpression in different cancers, and herein, the current study addressed this issue by revealing that TMAO could increase HULC levels significantly. It is important to place the 300 μ M TMAO concentration used in this study in its proper physiological context. While this concentration is higher than typical fasting systemic plasma levels in humans, which are generally in the low micromolar range (2-10 μ M), our in vitro model is designed to simulate the local colonic microenvironment. The colon is the primary site of microbial production of trimethylamine (TMA), the direct precursor to TMAO from dietary components like choline and carnitine. Local concentrations of these microbial metabolites within the gut lumen, before absorption, systemic dilution, and first-pass metabolism by the liver, can be orders of magnitude higher than what is measured in the blood (7, 9, 42). Therefore, using a high micromolar concentration like 300 μ M is a pathologically relevant approach to investigate the molecular effects of high TMAO precursor exposure on the intestinal epithelium, as might be seen with a diet linked to increased CRC risk.

Our analysis has identified a novel molecular axis in CRC cells, showing that TMAO-induced HULC expression is strongly associated with the overexpression of miR-21-5p and miR-200a-3p. Our analysis revealed a molecular mechanism for HULC role in CRC cells, showing that TMAO-induced HULC expression leads to the overexpression of miR-21-5p and miR-200a-3p. Given that these miRNAs are established drivers of oncogenic signaling, our findings suggest a pathway by which TMAO could enhance the molecular tumorigenic profile of CRC cells. miR-21 and miR-200 are two important miRNAs which based on published studies they play remarkable roles in cancer development, especially CRC metastasis.

Previous studies showed that miR-21 causes cell growth and metastasis in CRC cells through PTEN inhibition (43). Another study highlighted miR-21 in cancer progression via integrin- β 4 (ITG β 4) (44). However, the miR-200 role in cancers is controversial. Pichler et al. indicated that miR-200 has an anti-tumor function by EMT inhibition in CRC cells (45). While Humfries et al. reported that miR-200 is associated with the metastatic activity of cancer cells (46).

miRNAs are recognized for their significant role in regulating gene expression, primarily through their negative impact on gene expression. However, the regulatory mechanisms governing their own expression are complex and multifaceted. Several studies have shown that the expression of miR-21 can be regulated through the NF- κ B and ERK/MAPK signaling pathways (47, 48). P Dong et al. demonstrated that the p53 signaling pathway regulates the expression level of the miR-200 family, notably miR-200c, which is pivotal in controlling the EMT and maintaining stem cell-like characteristics (49). In a study conducted by Díez-Ricote et al., TMAO was found to significantly upregulate miR-21-5p expression in cellular models of liver and macrophages (50). The molecular mechanisms governing the expression of these miRNAs are complex. For instance, miR-21 expression can be regulated by NF- κ B and ERK/MAPK signaling. Given the established links in the literature between HULC and the p38MAPK pathway, we propose a hypothetical model where this pathway acts as a mediator of the effects we observed. In this model, TMAO-induced HULC could modulate p38MAPK activity, which in turn leads to the upregulation of miR-21-5p and miR-200a-3p.

However, we must explicitly state that the involvement of the p38MAPK pathway is speculative and was not directly investigated in this study. Our work demonstrates the TMAO-HULC-miRNA axis, but direct evidence, such as western blot analysis for phosphorylated p38 or the use of specific pathway inhibitors, would be required to confirm this proposed downstream mechanism. Therefore, while our data provide the basis for this hypothesis, further research is needed to dissect the precise intracellular signaling cascade. In contrast to the effects on miR-21-5p and miR-200a-3p, the expression of the tumor-suppressive miR-34a-5p was unaffected by either TMAO or HULC knockdown. While this finding differs from a previous report (51) potentially due to the use of different cell

models, this null result is highly informative for our study. The most compelling reason is likely cell-type specificity. The regulation of miR-34a-5p is highly context-dependent(52) and is famously controlled by the p53 tumor suppressor pathway(53). Caco-2 cells are known to have a null mutation for p53(54), rendering this key regulatory pathway non-functional. It is plausible that the TMAO-induced changes to miR-34a-5p observed previously occurred in a cell model with intact p53 signaling. Other plausible reasons relate to experimental kinetics.

It is possible that the dose (300 μ M) or timing (24 hours) used in this study, while effective for modulating the HULC axis, was not optimal for inducing a miR-34a-5p response in this specific cell line. The regulation of miR-34a-5p could be a more transient event or could follow different dose-response kinetics. Ultimately, this null result strengthens our study, as it provides strong evidence for the specificity of the pathway we have uncovered, suggesting that TMAO does not cause a global miRNA dysregulation but acts through HULC to influence a select group of miRNAs. miR-34 has anti-tumor properties(55, 56); therefore, we assumed that TMAO might not result in CRC oncogenic signaling cascade, and it might play a dual role in cancer by elevating miR-34. Our result did not support this point, and miR-34 was not changed upon TMAO treatment or HULC(KD). This may be due to the different primary cell lines used.

A critical point of this study is the distinction between the associative relationships we have identified and the direct causal mechanisms, which remain to be elucidated. Our data demonstrate that TMAO exposure is associated with increased HULC expression, which in turn correlates with elevated levels of miR-21-5p and miR-200a-3p. However, these findings represent a mechanistic gap. We did not perform experiments to prove that HULC directly binds to these miRNAs or their promoters, nor did we test the activity of intermediary signaling proteins like p38 MAPK. Therefore, the primary strength of this study is the identification of a novel, multi-component biological axis.

Future studies employing techniques such as luciferase reporter assays to test promoter activity, RNA immunoprecipitation (RIP) to assess direct binding, chromatin immunoprecipitation (ChIP) to identify transcription factors, and the use of specific pathway inhibitors are all essential next steps to bridge

this mechanistic gap and establish definitive causality. While Caco-2 cells serve as a valuable and widely used in vitro model for studying intestinal epithelial responses, a significant limitation of this study is the reliance on a single colorectal cancer cell line.

Findings from a single cell line may not fully represent the diversity of CRC and its responses to environmental factors like TMAO. For this initial investigation, Caco-2 provided a suitable established system to explore the fundamental principles of the proposed TMAO-HULC-miR-21-5p/200a-3p axis. However, future research is crucial to validate these findings in a panel of diverse CRC cell lines with varying genetic profiles and differentiation states, as well as more complex models such as patient-derived organoids or xenografts, and ultimately, in clinical cohorts. This broader approach will help confirm the generalizability of our results and provide a more comprehensive understanding of the context-dependent effects of TMAO and HULC in CRC pathogenesis

Furthermore, the use of a single TMAO concentration (300 μ M) at a single time point (24 hours). The primary objective of this investigation was not to perform a comprehensive kinetic analysis, but rather to provide the first 'proof-of-concept' evidence for the existence of a regulatory axis between TMAO and the lncRNA HULC, and to identify its downstream miRNA targets in colorectal cancer cells. Having established this novel pathway, we fully agree that future studies are now essential to characterize its dynamics. Such work should include a comprehensive dose-response analysis to determine the minimal effective TMAO concentration required for HULC induction. Additionally, a time-course experiment is needed to elucidate the temporal dynamics of this response. Therefore, while our study provides a critical, foundational observation, the precise dose- and time-dependent nature of the TMAO-HULC axis remains a key area for future investigation.

In addition, building upon the limitation of using a single cancer cell line to represent the heterogeneity of CRC, it also remains to be determined whether the observed upregulation of HULC, miR-21-5p, and miR-200a-3p upon TMAO treatment is specific to colorectal cancer cells or if similar effects occur in normal colon epithelial cells. Our current findings in the Caco-2 cancer cell line, coupled with the documented roles of HULC, miR-21-5p, and miR-200a-3p in regulatory

network associated with cancer(57, 58), suggest that these effects may be particularly relevant to cancer progression. However, without evaluating TMAO's impact on these molecules in normal colon epithelial cells, we cannot definitively conclude the cancer-specificity of these regulatory events. Future studies employing normal colon cell models are essential to clarify whether these TMAO-induced changes are part of a broader, non-cancer-specific response of the colon epithelium, or if they are selectively amplified or initiated within the cancerous state, thereby specifically contributing to tumorigenesis.

Our study demonstrates that TMAO upregulates HULC, leading to altered expression of miR-21-5p and miR-200a-3p, while the precise mechanisms underlying this regulation remain to be fully elucidated. Dissecting the detailed molecular cascade responsible for TMAO-induced HULC upregulation was beyond the immediate scope of this preliminary study, which primarily aimed to establish the existence of this regulatory axis.

A key finding of our study is that HULC knockdown reverses the TMAO-induced upregulation of miR-21-5p and miR-200a-3p. While this strongly suggests that HULC positively influences their expression, the precise regulatory mechanism was not determined. It is plausible that this regulation is indirect, occurring through HULC influence on shared signaling pathways rather than direct binding.

We propose several potential indirect mechanisms. First, as a lncRNA, HULC may modulate the activity of transcription factors that control the expression of both miR-21-5p and miR-200a-3p. Given the known role of the p38MAPK and NF- κ B pathways in regulating these miRNAs, HULC could be acting upstream within this cascade. Second, HULC could function as a molecular scaffold, enhancing the signaling that leads to miRNA transcription. Finally, HULC might also influence the post-transcriptional processing of pri-miRNA into mature, functional miRNAs. Further studies, such as chromatin immunoprecipitation (ChIP) to assess transcription factor binding, are needed to elucidate this specific molecular link.

In conclusion, our in vitro study demonstrates that TMAO upregulates HULC expression in Caco-2 colorectal cancer cells, leading to the elevated expression of oncogenic miRNAs, miR-21-5p and miR-200a-3p. These findings identify a novel TMAO-

HULC-miRNA regulatory axis that may be involved in pro-tumorigenic signaling in CRC. While these results highlight a potential mechanism for TMAO role in cancer, they are based on molecular changes in a single cell line. It is crucial to emphasize that these conclusions are drawn from a single cell line and do not account for the known heterogeneity of CRC. Therefore, direct functional consequences on CRC progression require further investigation in more complex models. Future studies should aim to validate these findings and explore their functional impact on cell proliferation, migration, and in vivo tumor growth.

Study Limitations and Future Directions

It is essential to interpret the findings of this study within the context of its limitations, which frame it as an exploratory, hypothesis-generating work. The primary limitations are threefold. First, our observations are derived exclusively from a single cancer cell line (in vitro), and given the well-known heterogeneity of CRC, these findings require validation in a broader panel of CRC cell lines and, ideally, in non-transformed colonic epithelium to assess cancer-specificity. Second, our data establishes a strong molecular association but lacks direct mechanistic proof; the causal links between HULC, downstream signaling pathways, and miRNA expression remain to be definitively proven.

Third, this study did not include functional assays to connect the observed molecular changes to a cancer phenotype like proliferation or migration. Therefore, any inference of in vivo or clinical relevance is premature. Our future work will directly address these limitations by: (i) validating this axis in diverse CRC cell lines and patient-derived organoids; (ii) performing mechanistic experiments to establish causality; and (iii) conducting functional assays to determine the biological consequences of the TMAO-HULC axis.

Acknowledgements

This work as a Master thesis was financially supported by a grant received from Vice- Chancellery for Research of Kurdistan University of Medical Sciences (IR.MUK.REC.14.1.343). The authors thank the Cellular and Molecular Research Laboratories of School of Medicine of Kurdistan University of Medical Sciences.

References

1. Xi Y, Xu P. Global colorectal cancer burden in 2020 and projections to 2040. *Transl Oncol.* 2021;14(10):101174.
2. Siegel RL, Miller KD, Goding Sauer A, Fedewa SA, Butterly LF, Anderson JC, et al. Colorectal cancer statistics, 2020. *CA: Cancer J Clin.* 2020;70(3):145-164.
3. Anbari K, Ghanadi K. Colorectal Cancer: Risk Factors, Novel Approaches in Molecular Screening and Treatment. *Int J Mol Med.* 2025;14(1):576.
4. Hossain MS, Karuniawati H, Jairoun AA, Urbi Z, Ooi DJ, John A, et al. Colorectal cancer: a review of carcinogenesis, global epidemiology, current challenges, risk factors, preventive and treatment strategies. *Cancers.* 2022;14(7):1732.
5. Peng Z, Wang C-X, Fang E-H, Wang G-B, Tong Q. Role of epithelial-mesenchymal transition in gastric cancer initiation and progression. *World J Gastroenterol.* 2014;20(18):5403.
6. Zhu Q-C, Gao R-Y, Wu W, Qin H-L. Epithelial-mesenchymal transition and its role in the pathogenesis of colorectal cancer. *Asian Pac J Cancer Prev.* 2013;14(5):2689-98.
7. Chan CWH, Law BMH, Waye MMY, Chan JYW, So WKW, Chow KM. Trimethylamine-N-oxide as one hypothetical link for the relationship between intestinal microbiota and cancer-where we are and where shall we go? *J Cancer.* 2019;10(23):5874.
8. Liu Y, Dai M. Trimethylamine N-oxide generated by the gut microbiota is associated with vascular inflammation: new insights into atherosclerosis. *Mediators Inflamm.* 2020;2020.
9. Ufnal M, Zadlo A, Ostaszewski R. TMAO: A small molecule of great expectations. *Nutrition.* 2015;31(11-12):1317-23.
10. Zhang W, An Y, Qin X, Wu X, Wang X, Hou H, et al. Gut microbiota-derived metabolites in colorectal cancer: the bad and the challenges. *Front Oncol.* 2021;11:739648.
11. Lai Y, Tang H, Zhang X, Zhou Z, Zhou M, Hu Z, et al. Trimethylamine-N-oxide aggravates kidney injury via activation of p38/MAPK signaling and upregulation of HuR. *Kidney Blood Press Res.* 2022;47(1):61-71.
12. Duan Q, Cai L, Zheng K, Cui C, Huang R, Zheng Z, et al. lncRNA KCNQ1OT1 knockdown inhibits colorectal cancer cell proliferation, migration and invasiveness via the PI3K/AKT pathway. *Oncol Lett.* 2020;20(1):601-10.
13. Mattick JS, Amaral PP, Carninci P, Carpenter S, Chang HY, Chen L-L, et al. Long non-coding RNAs: definitions, functions, challenges and recommendations. *Nat Rev Mol Cell Biol.* 2023;24(6):430-47.
14. Yu S-y, Dong B, Tang L, Zhou S-h. lncRNA MALAT1 sponges miR-133 to promote NLRP3 inflammasome expression in ischemia-reperfusion injured heart. *Int J Cardiol.* 2018;254:50.
15. Xiong W, Huang C, Deng H, Jian C, Zen C, Ye K, et al. Oncogenic non-coding RNA NEAT1 promotes the prostate cancer cell growth through the SRC3/IGF1R/AKT pathway. *Int J Biochem Cell Biol.* 2018;94:125-32.
16. Zhu H, Zheng T, Yu J, Zhou L, Wang L. lncRNA XIST accelerates cervical cancer progression via upregulating Fus through competitively binding with miR-200a. *Biomed Pharmacother.* 2018;105:789-97.
17. Duan Y, Fang Z, Shi Z, Zhang L. Knockdown of lncRNA CCEPR suppresses colorectal cancer progression. *Exp Ther Med.* 2019;18(5):3534-42.
18. Jin C, Shi W, Wang F, Shen X, Qi J, Cong H, et al. Long non-coding RNA HULC as a novel serum biomarker for diagnosis and prognosis prediction of gastric cancer. *Oncotarget.* 2016;7(32):51763.
19. Sun X-H, Yang L-B, Geng X-L, Wang R, Zhang Z-C. Increased expression of lncRNA HULC indicates a poor prognosis and promotes cell metastasis in osteosarcoma. *Int J Clin Exp Pathol.* 2015;8(3):2994.
20. Yang X-J, Huang C-Q, Peng C-W, Hou J-X, Liu J-Y. Long noncoding RNA HULC promotes colorectal carcinoma progression through epigenetically repressing NKD2 expression. *Gene.* 2016;592(1):172-8.
21. Shen X, Guo H, Xu J, Wang J. Inhibition of lncRNA HULC improves hepatic fibrosis and hepatocyte apoptosis by inhibiting the MAPK signaling pathway in rats with nonalcoholic fatty liver disease. *J Cell Physiol.* 2019;234(10):18169-79.
22. Shukla GC, Singh J, Barik S. MicroRNAs: processing, maturation, target recognition and regulatory functions. *Mol Pharmacol.* 2011;3(3):83.

23. O'Brien J, Hayder H, Zayed Y, Peng C. Overview of microRNA biogenesis, mechanisms of actions, and circulation. *Front Endocrinol.* 2018;9:388354.
24. Basiri P, Afshar S, Amini R, Soltanian AR, Saidijam M, Mahdavinezhad A. Evaluation of miR-330-3p and BMI1 Expression in Colorectal Cancer Patients, Healthy Adjacent Tissues, and Polypoid Adenomatous Lesions. *Int J Mol Med.* 2022;11(4):334.
25. You C, Jin L, Xu Q, Shen B, Jiao X, Huang X. Expression of miR- 21 and miR- 138 in colon cancer and its effect on cell proliferation and prognosis. *Oncol Lett.* 2019;17(2):2271-7.
26. Yang Y, Ma Y, Shi C, Chen H, Zhang H, Chen N, et al. Overexpression of miR-21 in patients with ulcerative colitis impairs intestinal epithelial barrier function through targeting the Rho GTPase RhoB. *Biochem Biophys Res Commun.* 2013;434(4):746-52.
27. Yang L, Wang B, Zhou Q, Wang Y, Liu X, Liu Z, et al. MicroRNA-21 prevents excessive inflammation and cardiac dysfunction after myocardial infarction through targeting KBTBD7. *Cell Death Dis.* 2018;9(7):769.
28. He F, Xiao Z, Yao H, Li S, Feng M, Wang W, et al. The protective role of microRNA-21 against coxsackievirus B3 infection through targeting the MAP2K3/P38 MAPK signaling pathway. *J Transl Med.* 2019;17:1-11.
29. Li Y, Sun J, Cai Y, Jiang Y, Wang X, Huang X, et al. MiR-200a acts as an oncogene in colorectal carcinoma by targeting PTEN. *Exp Mol Pathol.* 2016;101(3):308-13.
30. Lai M, Du G, Shi R, Yao J, Yang G, Wei Y, et al. MiR-34a inhibits migration and invasion by regulating the SIRT1/p53 pathway in human SW480 cells. *Mol Med Rep.* 2015;11(5):3301-7.
31. Gao J, Li N, Dong Y, Li S, Xu L, Li X, et al. miR-34a-5p suppresses colorectal cancer metastasis and predicts recurrence in patients with stage II/III colorectal cancer. *Oncogene.* 2015;34(31):4142-52.
32. Bahramirad Z, Moloudi MR, Moradzad M, Abdollahi A, Vahabzadeh Z. Trimethylamine-N-oxide, a New Risk Factor for Non-alcoholic Fatty Liver Disease Changes the Expression of miRNA-34a, and miRNA-122 in the Fatty Liver Cell Model. *Biochem Genet.* 2025;63(2):1298-309.
33. Hakhamaneshi MS, Abdolahi A, Vahabzadeh Z, Abdi M, Andalibi P. Toll-like receptor 4: a macrophage cell surface receptor is activated by trimethylamine-N-oxide. *Cell J (Yakhteh).* 2021;23(5):516.
34. Apostolopoulos A, Kawamoto N, Chow SYA, Tsuiji H, Ikeuchi Y, Shichino Y, et al. dCas13-mediated translational repression for accurate gene silencing in mammalian cells. *Nat Commun.* 2024;15(1):2205.
35. Shi P, Murphy MR, Aparicio AO, Kesner JS, Fang Z, Chen Z, et al. Collateral activity of the CRISPR/RfxCas13d system in human cells. *Commun Biol.* 2023;6(1):334.
36. Moradzad M, Moloudi MR, Abdollahi A, Fakhari S, Vahabzadeh Z. TMAO promotes metabolic dysfunction-associated fatty liver disease (MAFLD) development through long-non coding RNA-highly upregulated liver cancer (HULC) lncRNA HULC contribution in MAFLD development. *J Diabetes Metab Dis.* 2025;24(1):131.
37. Yang S, Dai H, Lu Y, Li R, Gao C, Pan S. Trimethylamine N- oxide promotes cell proliferation and angiogenesis in colorectal cancer. *J Immunol Res.* 2022;2022(1):7043856.
38. Wu Y, Rong X, Pan M, Wang T, Yang H, Chen X, et al. Integrated analysis reveals the gut microbial metabolite TMAO promotes inflammatory hepatocellular carcinoma by upregulating POSTN. *Front Cell Dev Biol.* 2022;10:840171.
39. Zhao Y, Guo Q, Chen J, Hu J, Wang S, Sun Y. Role of long non-coding RNA HULC in cell proliferation, apoptosis and tumor metastasis of gastric cancer: a clinical and in vitro investigation. *Oncol Rep.* 2014;31(1):358-64.
40. Liu T, Liu Y, Wei C, Yang Z, Chang W, Zhang X. LncRNA HULC promotes the progression of gastric cancer by regulating miR-9-5p/MYH9 axis. *Biomed Pharmacother.* 2020;121:109607.
41. Liu L, Zhou X-Y, Zhang J-Q, Wang G-G, He J, Chen Y-Y, et al. LncRNA HULC promotes non-small cell lung cancer cell proliferation and inhibits the apoptosis by up-regulating sphingosine kinase 1 (SPHK1) and its downstream PI3K/Akt pathway. *Eur Rev Med Pharmacol Sci.* 2018 ;22(24):8722-8730

42. Zeisel SH, Da Costa K-A. Choline: an essential nutrient for public health. *Nutr Rev.* 2009;67(11):615-23.
43. Wu Y, Song Y, Xiong Y, Wang X, Xu K, Han B, et al. MicroRNA-21 (Mir-21) promotes cell growth and invasion by repressing tumor suppressor PTEN in colorectal cancer. *Cell Physiol Biochem.* 2017;43(3):945-58.
44. Ferraro A, Kontos CK, Boni T, Bantounas I, Siakouli D, Kosmidou V, et al. Epigenetic regulation of miR-21 in colorectal cancer: ITGB4 as a novel miR-21 target and a three-gene network (miR-21-ITGB4-PDCD4) as predictor of metastatic tumor potential. *Epigenetics.* 2014;9(1):129-41.
45. Pichler M, Ress A, Winter E, Stiegelbauer V, Karbiener M, Schwarzenbacher D, et al. MiR-200a regulates epithelial to mesenchymal transition-related gene expression and determines prognosis in colorectal cancer patients. *Br J Cancer.* 2014;110(6):1614-21.
46. Humphries B, Yang C. The microRNA-200 family: small molecules with novel roles in cancer development, progression and therapy. *Oncotarget.* 2015;6(9):6472.
47. N Choudhury S, Li Y. miR-21 and let-7 in the Ras and NF-κB pathways. *Microna.* 2012;1(1):65-9.
48. Mao XH, Chen M, Wang Y, Cui PG, Liu SB, Xu ZY. MicroRNA- 21 regulates the ERK/NF- κB signaling pathway to affect the proliferation, migration, and apoptosis of human melanoma A375 cells by targeting SPRY1, PDCD4, and PTEN. *Mol Carcinogenesis.* 2017;56(3):886-94.
49. Dong P, Karaayvaz M, Jia N, Kaneuchi M, Hamada J, Watari H, et al. Mutant p53 gain-of-function induces epithelial–mesenchymal transition through modulation of the miR-130b–ZEB1 axis. *Oncogene.* 2013;32(27):3286-95.
50. Díez-Ricote L, Ruiz-Valderrey P, Micó V, Blanco-Rojo R, Tomé-Carneiro J, Dávalos A, et al. Trimethylamine n-oxide (TMAO) modulates the expression of cardiovascular disease-related microRNAs and their targets. *Int J Mol Sci.* 2021;22(20):11145.
51. Bahramirad Z, Moloudi MR, Moradzad M, Abdollahi A, Vahabzadeh Z. Trimethylamine-N-oxide, a New Risk Factor for Non-alcoholic Fatty Liver Disease Changes the Expression of miRNA-34a, and miRNA-122 in the Fatty Liver Cell Model. *Biochem Genet.* 2024;1-12.
52. Rokavec M, Li H, Jiang L, Hermeking H. The p53/miR-34 axis in development and disease. *J Mol Cell Biol.* 2014;6(3):214-30.
53. Okada N, Lin C-P, Ribeiro MC, Biton A, Lai G, He X, et al. A positive feedback between p53 and miR-34 miRNAs mediates tumor suppression. *Genes Dev.* 2014;28(5):438-50.
54. NR R, editor p53 mutations in colorectal cancer. *Natl Acad Sci USA;* 1990.
55. Ji Q, Hao X, Meng Y, Zhang M, DeSano J, Fan D, et al. Restoration of tumor suppressor miR-34 inhibits human p53-mutant gastric cancer tumorspheres. *BMC cancer.* 2008;8:1-12.
56. Ji Q, Hao X, Zhang M, Tang W, Yang M, Li L, et al. MicroRNA miR-34 inhibits human pancreatic cancer tumor-initiating cells. *PloS one.* 2009;4(8):e6816.
57. Pang Q, Huang S, Wang H, Cao J. HULC-IGF2BP2 Interaction Drives Proliferation and Metastasis in Colorectal Cancer. *J Cancer.* 2024;15(20):6686.
58. Tan L, Chen Z, Wang Y, Wang F. The expressions of miR-200a and miR-21 in colorectal cancer tissues and their effects on the biological functions of HCT116 cells. *Int J Mol Med.* 2020;13(3):1484-92.